Environmental properties of 6 cores in the λ Orionis cloud

Hee-Weon Yi[1], Jeong-Eun Lee[1], Tie Liu[2,3] , and Kee-Tae Kim[2]

1 School of Space Research,University of Kyung Hee
2 Korea Astronomy and Space Science Institute
3 East Asian Observatory, 660 N. A'ohoku Place, Hilo, HI 96720, USA

Radio User's Meeting

1. INTRODUCTION : Planck Galactic Cold Clumps (PGCCs)

PGCCs (Planck) : 13,188

TOP (TRAO) : 2,000 PI : Tie Liu

SCOPE (SCUBA-2) : 1,000

KVN

SMA

ALMA

Planck Galactic Cold Clumps (PGCCs) ?

-> Covering the whole sky

-> Probing widely different environments

-> Goldmine for investigations of the early phases of star formation

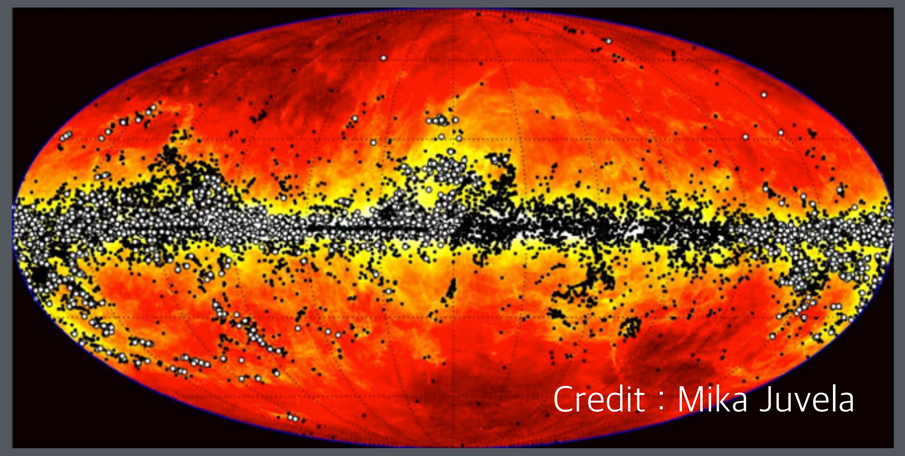

The λ Orionis cloud has much lower density, higher dust temperature, and lower dust emissivity spectral index β (from Planck measurements; Planck collaboration et al. 2015).

"How core formation depends on the physical conditions provided by the parent cloud?"

- 13,188 PGCC sources
- 2,000 proposed PGCC sources

https://topscope.asiaa.sinica.edu.tw/tiki/tiki-index.php

1. INTRODUCTION : Orion complex ; Orion A , Orion B and λ Orionis clouds

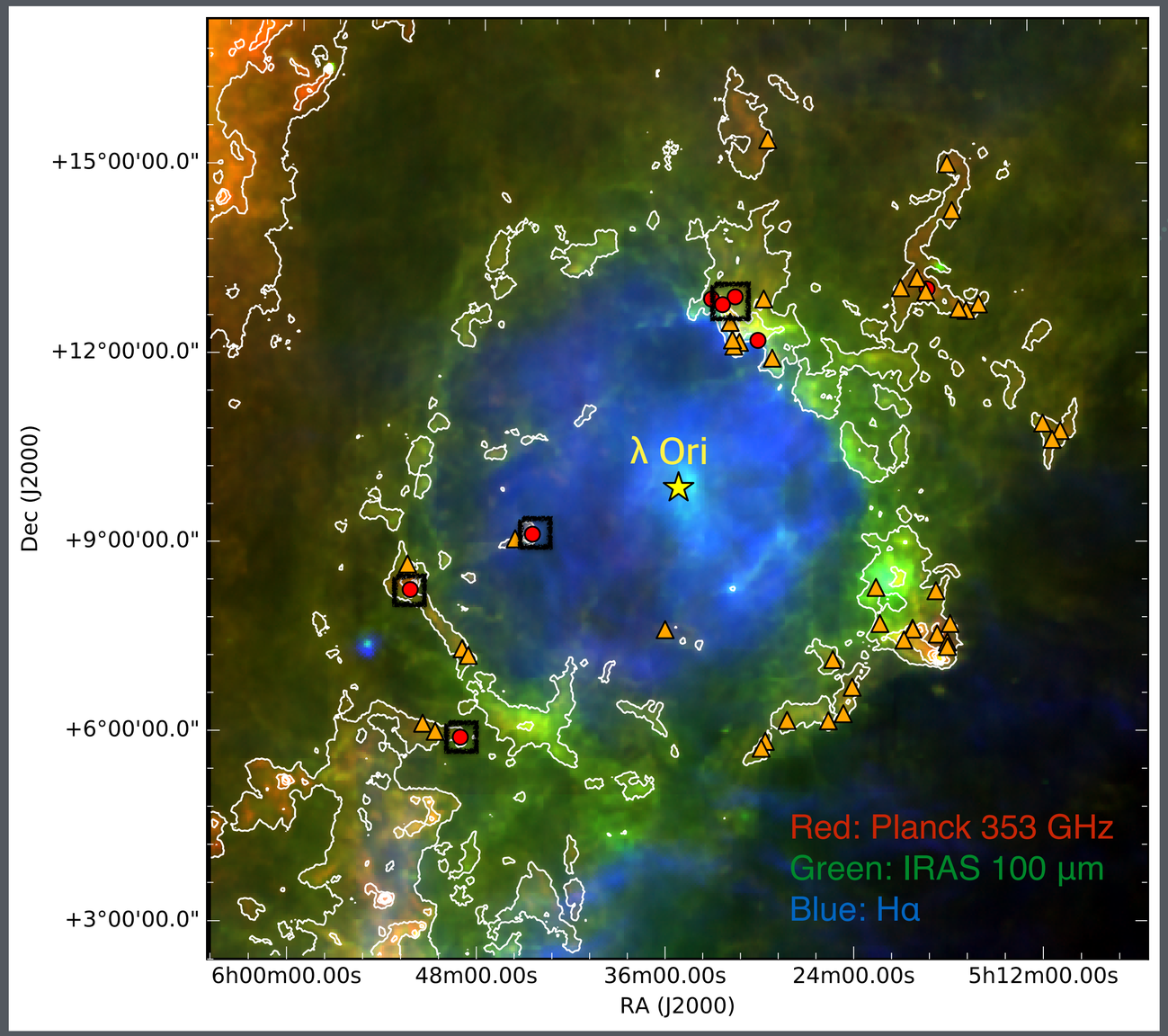

Large H II region

Distance : 380 pc derived by Hipparcos
Total mass : 1.4x10^4 M$_\odot$ Lang et al. 2000

50 PGCCs in the λ Orionis cloud

Column density > 5 x 10^{20} cm^{-2}

Supernova explosion ~ 1 Myr ago

OB association known as “λ Ori”

● : detected PGCCs at 850 μm
▲ : non-detected PGCCs at 850 μm

2.PREVIOUS RESULTS : Observation results of JCMT/SCUBA-2 - 8 PGCCs in the λ Orionis cloud

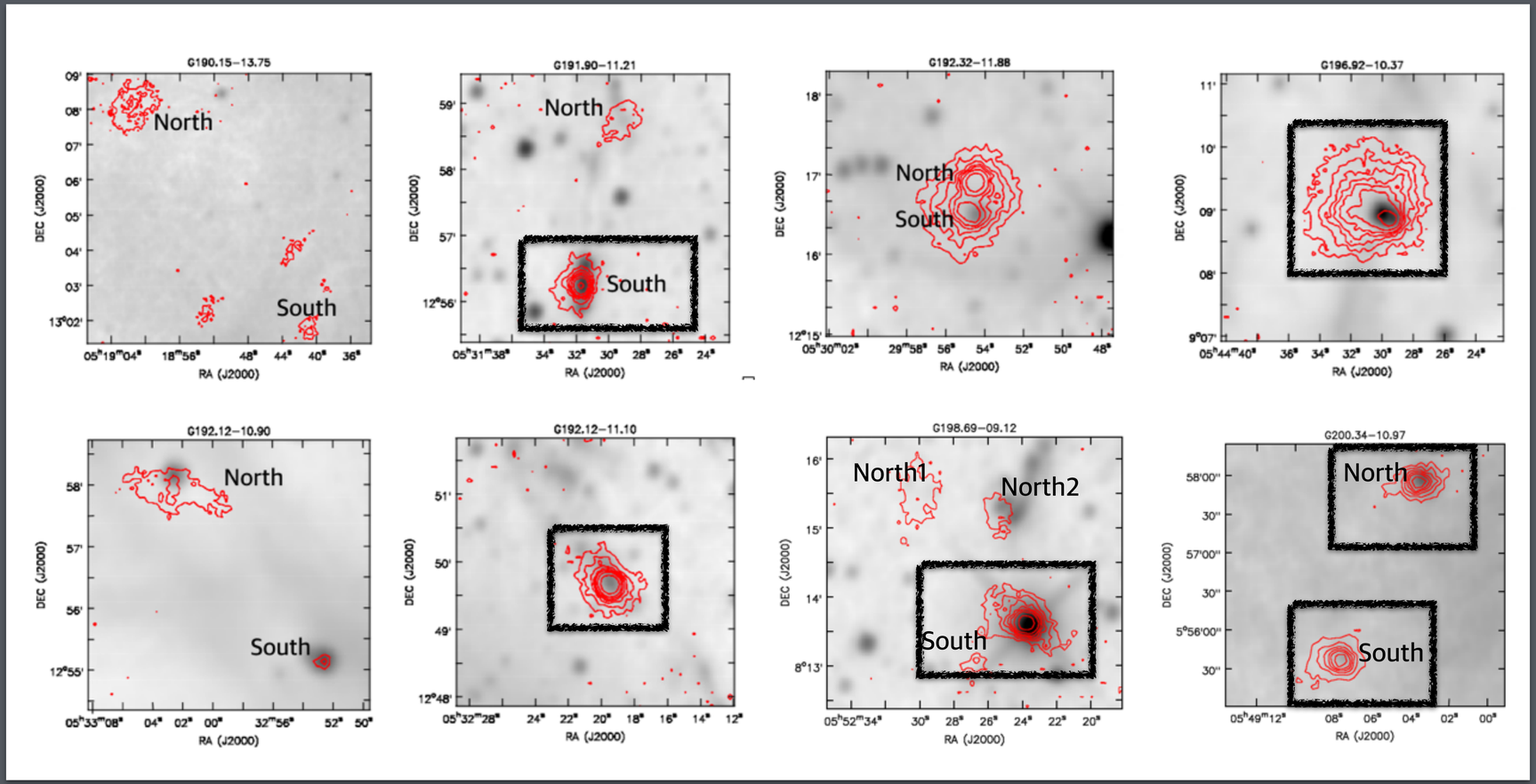

Contours : SCUBA-2 850 μm
Grey scale : WISE 12 μm

2. PREVIOUS RESULTS : 119 Dense cores and physical parameters

Median values of physical parameters of PGCCs

Cloud	l	b	Number (PGCC)	Mass (M⊙)	T_{dust} (K)	β	$N(H_2)$ ($10^{21}cm^{-2}$)	$n(H_2)$ ($10^{2}cm^{-3}$)
λ Orionis	[188,201]	[-18,-17]	177	4.9	16.1	1.65	3.2	2.2
Orion B	[201,210]	[-17,-5]	154	13.8	13.9	1.96	6.4	4.1
Orion A	[203,217]	[-21,-17]	135	7.7	13.4	2.08	10.9	6.6

Median values of physical parameters of cores

Cloud	l	b	Number (PGCC)	Number (core)	Size (pc)	Mass (M⊙)	$N(H_2)$ ($10^{22}cm^{-2}$)	$n(H_2)$ ($10^{5}cm^{-3}$)
λ Orionis	[190,201]	[-18,-10]	8	15	0.08	0.77	8.2	2.5
Orion B	[201,206]	[-17,-11]	9	30	0.10	1.81	38.4	15.8
Orion A	[207,216]	[-21,-17]	23	74	0.11	1.18	14.7	3.4

$$M = \frac{S_\nu D^2}{\kappa_\nu B_\nu(T)}$$

$$N_{H_2} = \frac{S'_\nu/\Omega}{\mu m_H B_\nu(T)\kappa_\nu}$$

3. RESULTS : Observation results of SMA (G191.90-11.21 S)

RA 05:31:31.604
DEC +12:56:15.134

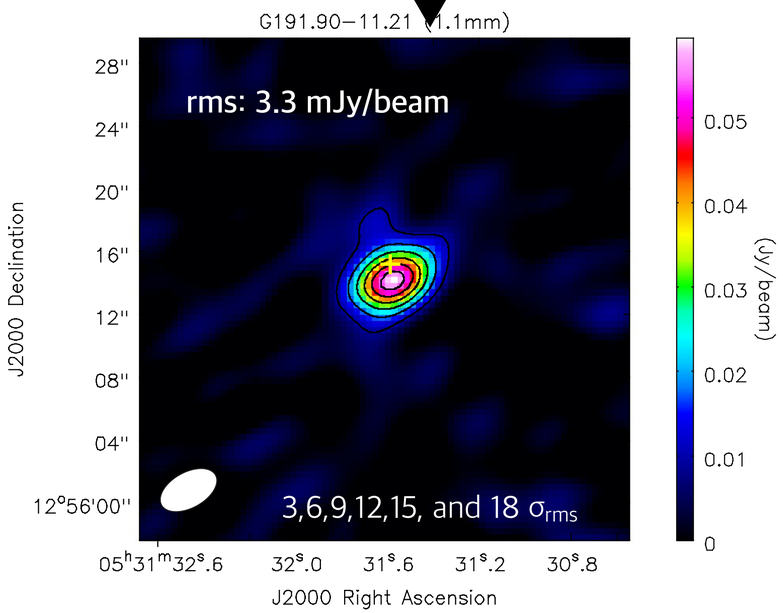

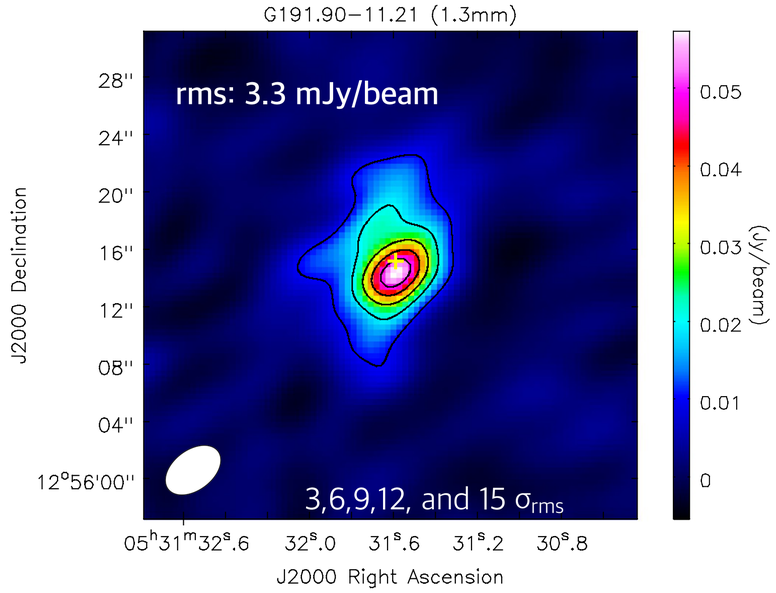

Class 0: $0.3 < \alpha_{4.5\text{-}24}$ and $70\ K < T_{bol}$

Class I: $0.3 < \alpha_{4.5\text{-}24}$ and $70\ K < T_{bol} < 650\ K$

Flat-spectrum: $-0.3 < \alpha_{4.5\text{-}24} < 0.3$

Class II: $-0.3 < \alpha_{4.5\text{-}24}$ and $650\ K < T_{bol}$

Furlan et al. 2016

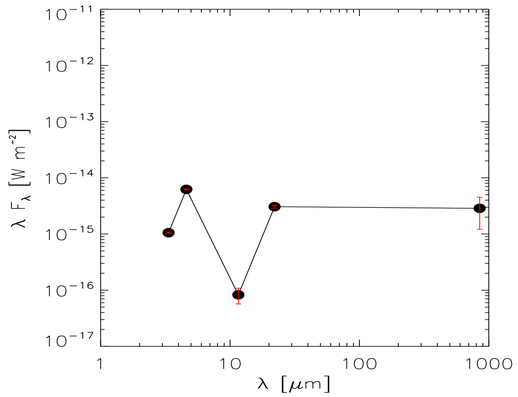

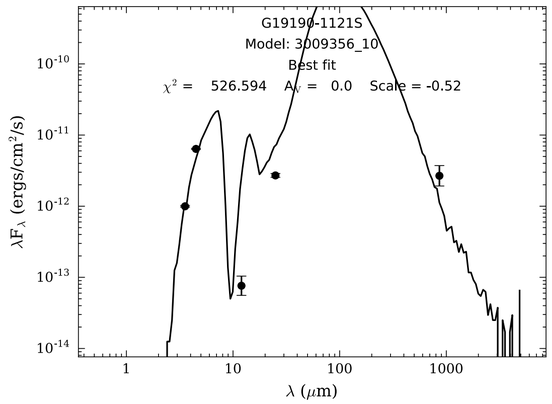

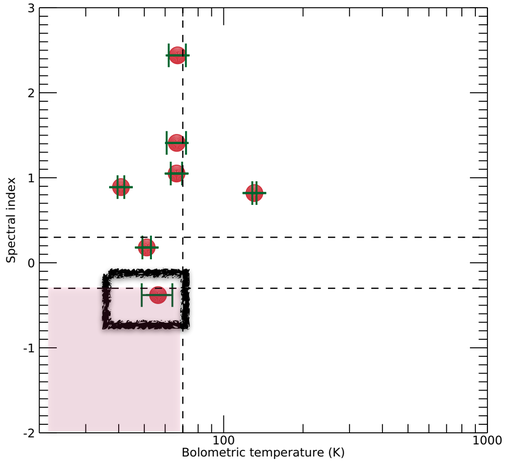

The 3.6–22 μm spectral index $\alpha_{3.6\text{–}22}$ versus the bolometric temperature (T_{bol}) are plotted for the 7 YSOs in our sample.

mass (M⊙)	N(H_2) (cm^{-2})	L_{bol} (L⊙)	L_{bol} (SED fitter)	T_{bol} (K)	α	Class	β	t (SED fitter)
0.89	11.8	0.3±0.1	3.7	56.4±7.5	-0.38	**0**	1.51	3,511

3. RESULTS : Observation results of SMA (G192.12-11.10)

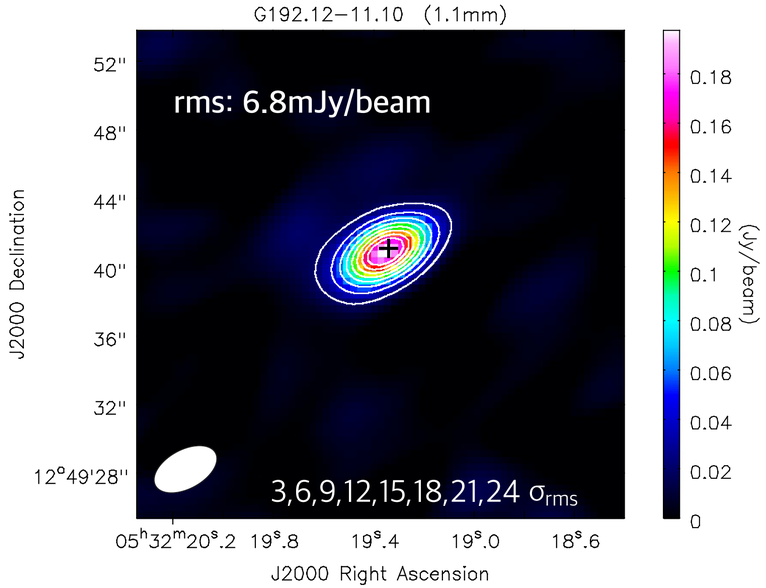

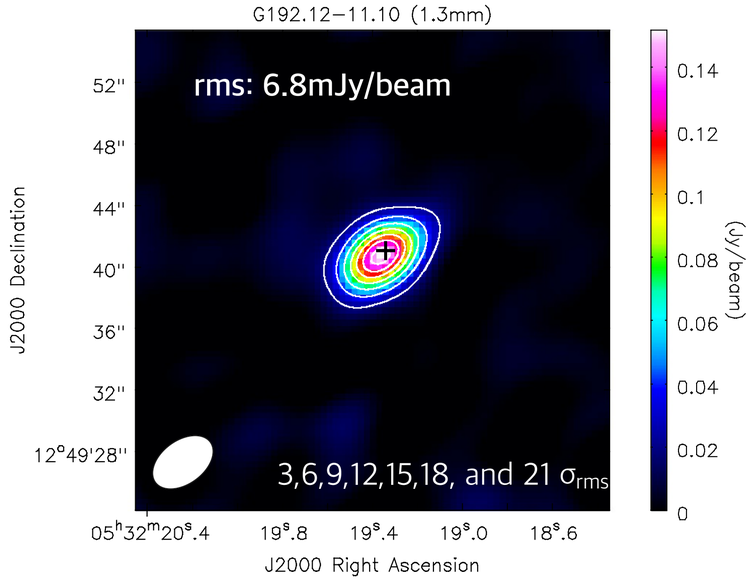

RA 05:32:19.361
DEC +12:49:40.756

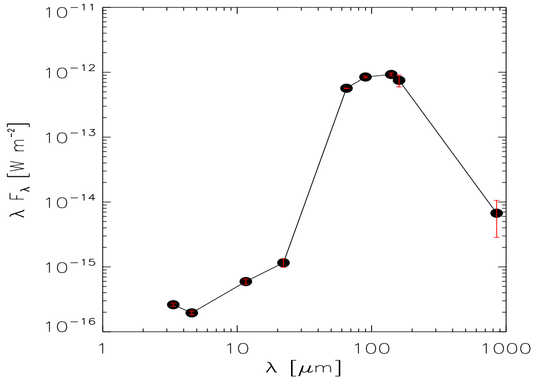

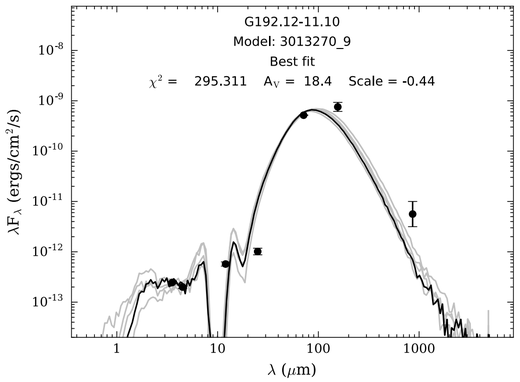

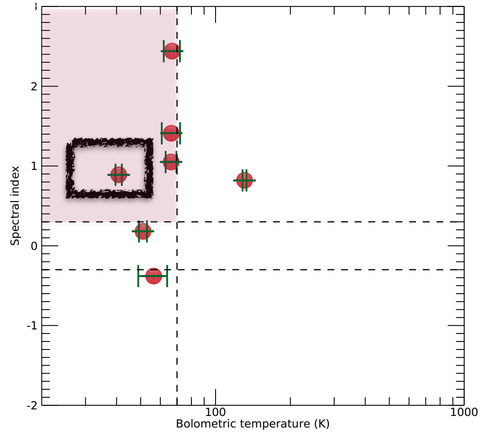

mass (M⊙)	N(H_2) (10^{24} cm^{-2})	L_{bol} (L⊙)	L_{bol} (SED fitter)	T_{bol} (K)	α	Class	β	t (SED fitter)
1.06	13.7	7.4±0.5	4.8	40.9±1.2	0.89	**0**	0.88	22,600

3. RESULTS : Observation results of SMA (G196.92-10.37)

05:44:29.239 +09:08:52.060
05:44:30.010 +09:08:56.833

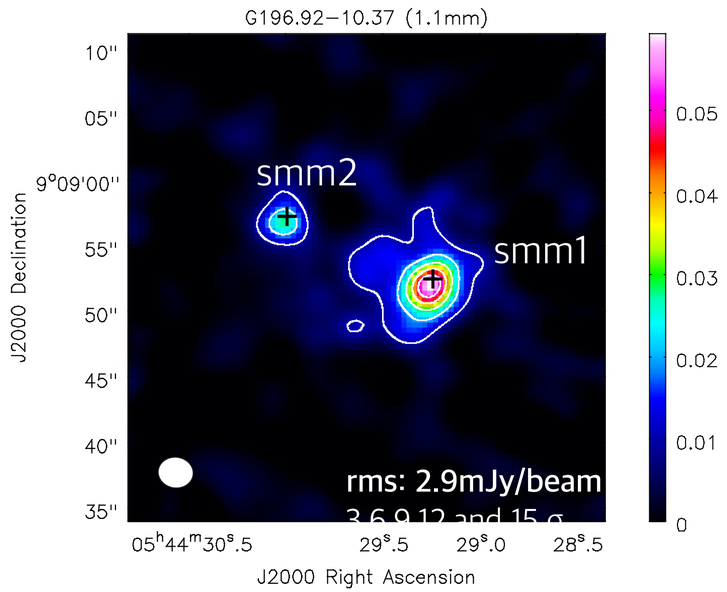

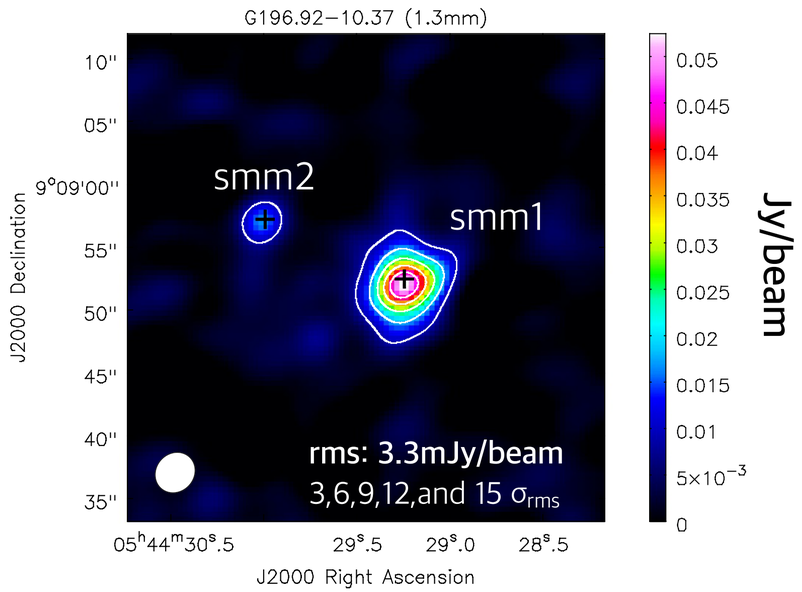

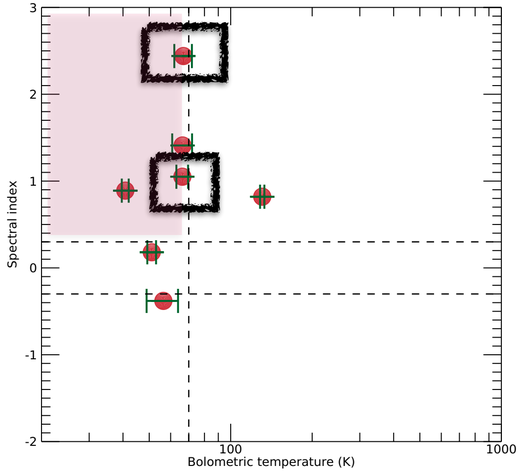

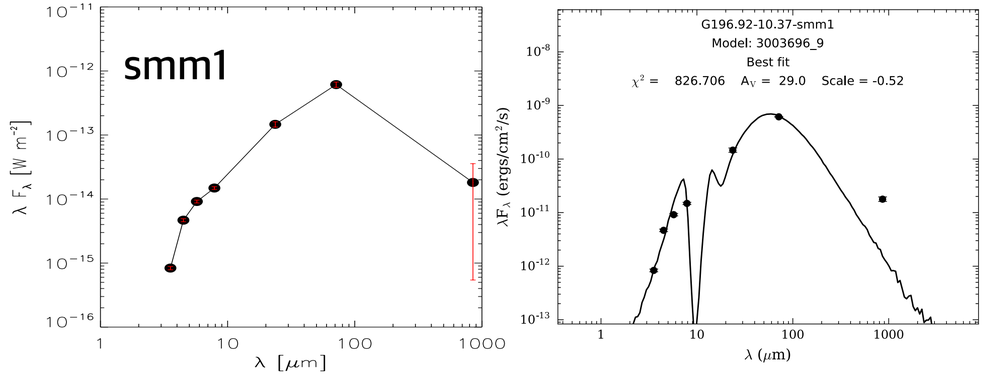

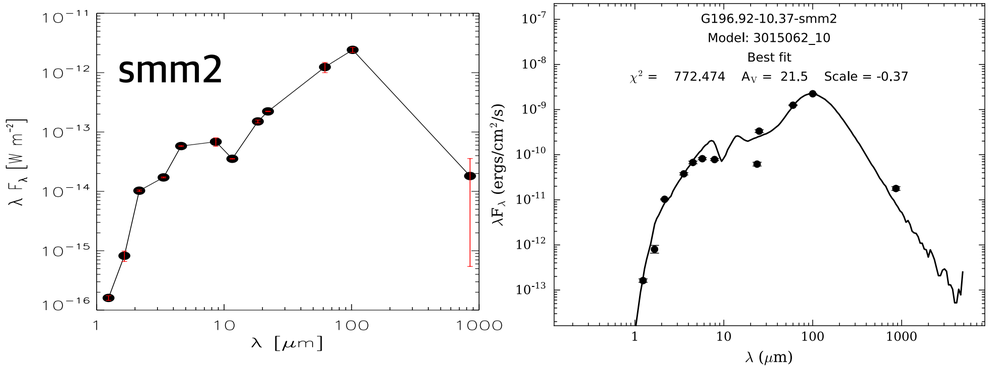

source	mass (M⊙)	N(H_2) (cm^{-2})	L_{bol} ($L_⊙$)	L_{bol} (SED fitter)	T_{bol} (K)	α	Class	β	t (SED fitter)
G196-smm1	0.58	7.6	5.5±0.9	2.9	66.9±5.0	2.44	**0**	1.72	2,695
G196-smm2	0.11	1.1	15.9±2.4	15.4	66.3±3.3	1.05	**0**	2.84	2,578

3. RESULTS : Observation results of SMA (G198.69-09.12 S)

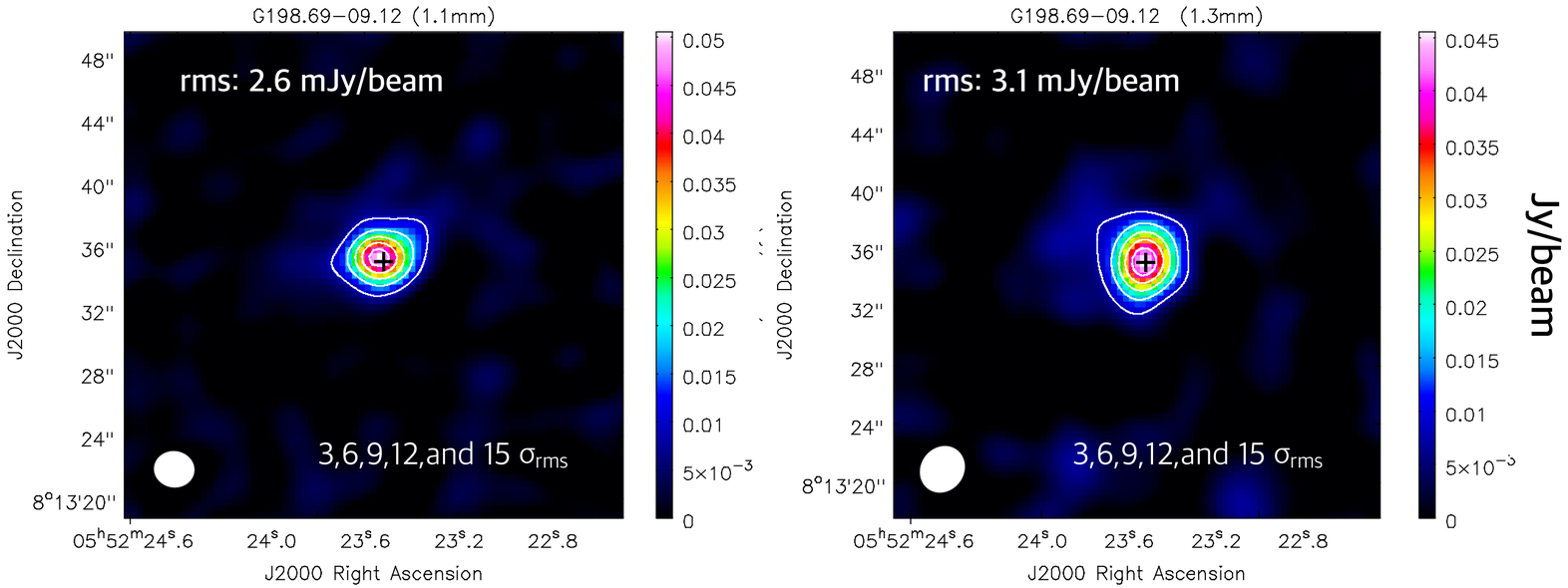

RA 05:52:23.527
DEC +08:13:35.177

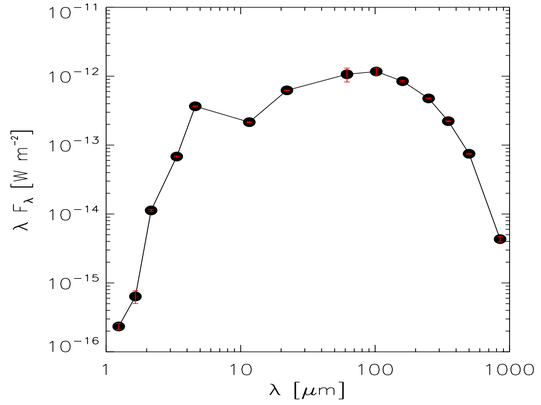

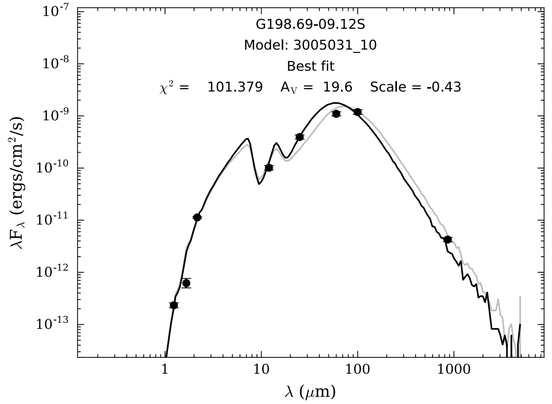

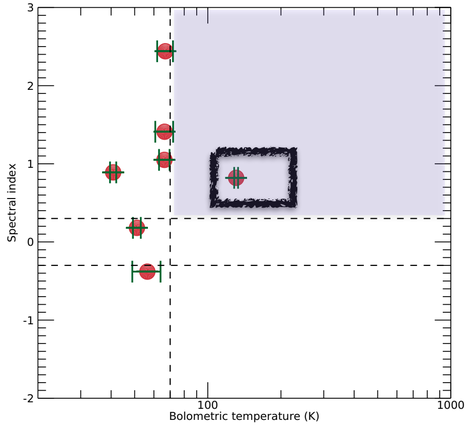

mass (M⊙)	N(H_2) (cm^{-2})	L_{bol} (L⊙)	L_{bol} (SED fitter)	T_{bol} (K)	α	Class	β	t (SED fitter)
0.55	7.2	15.3±1.7	8.3	130.8±2.4	0.82	I	0.90	22,090

3. RESULTS : Observation results of SMA (G200.34-10.97 N)

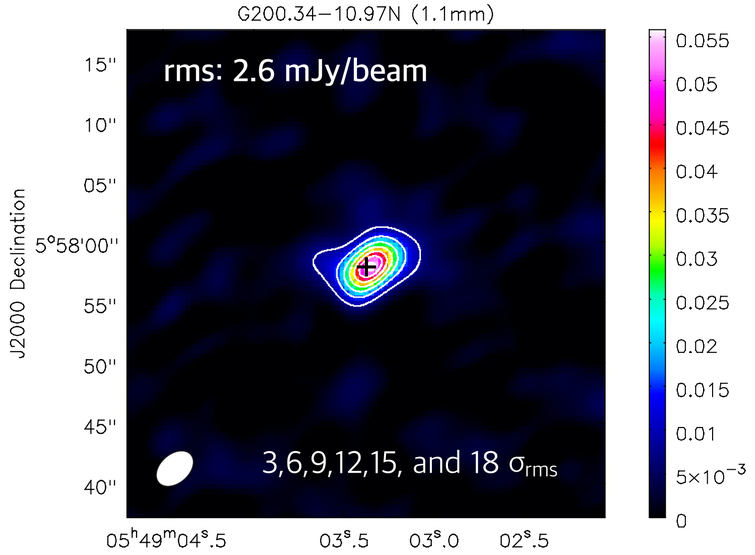

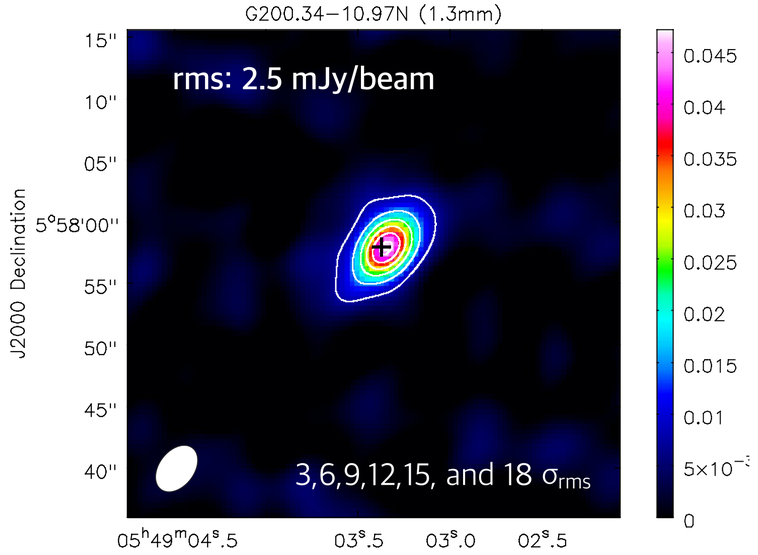

RA 05:49:03.345
DEC +05:57:58.022

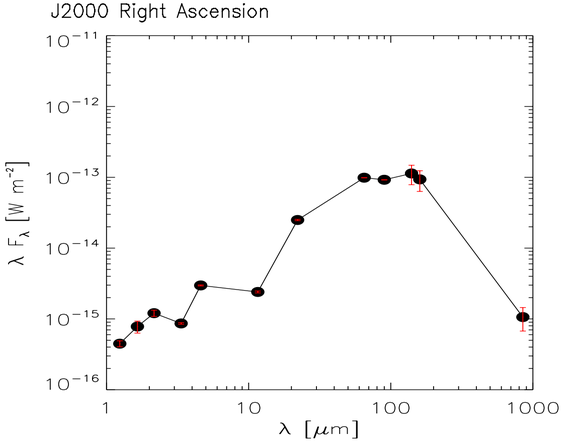

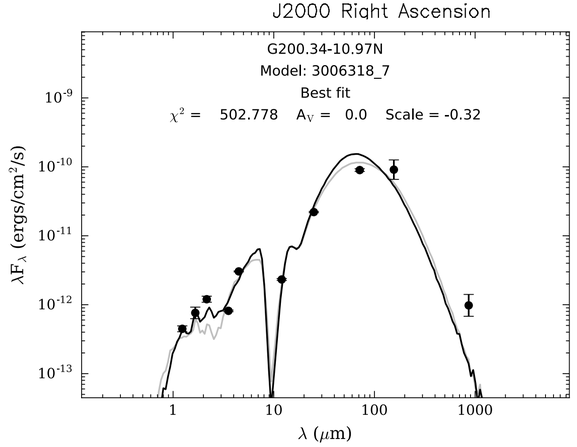

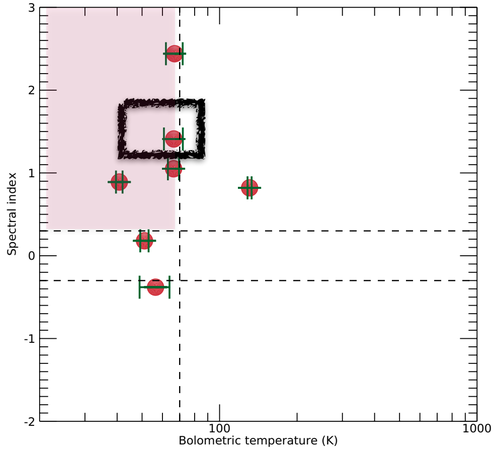

mass (M⊙)	N(H_2) (cm^{-2})	L_{bol} (L⊙)	L_{bol} (SED fitter)	T_{bol} (K)	α	Class	β	t (SED fitter)
0.48	6.4	1.2±0.1	1.2	66.4±5.6	1.41	**0**	1.54	3,994

3. RESULTS : Observation results of SMA (G200.34-10.97 S)

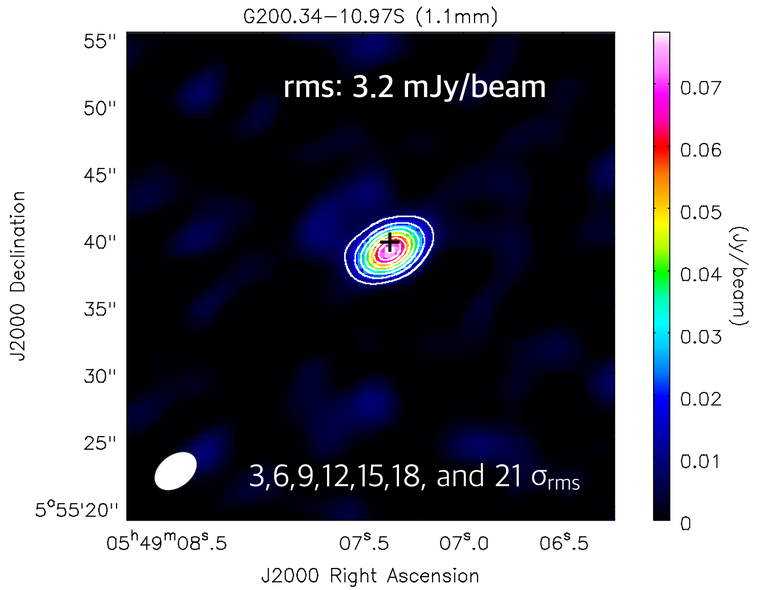

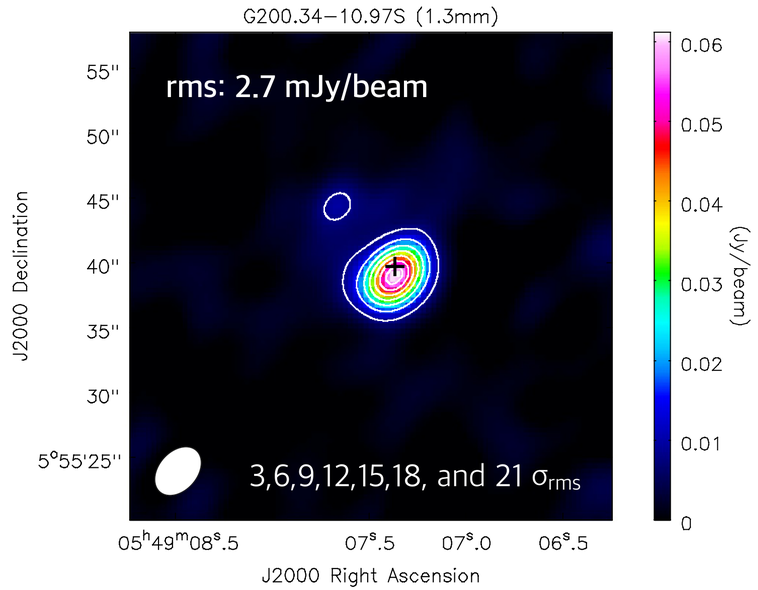

RA 05:49:07.367
DEC +05:55:39.098

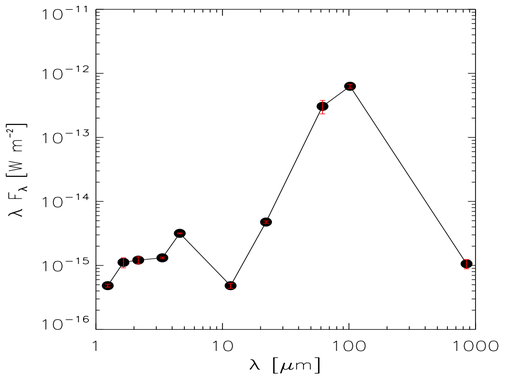

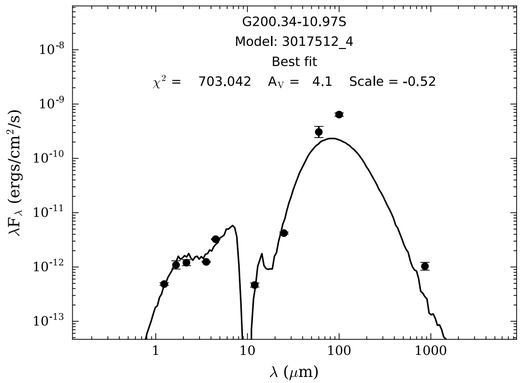

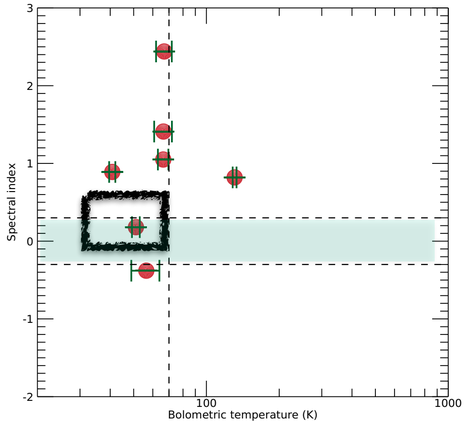

mass (M⊙)	N(H_2) (cm^{-2})	L_{bol} (L⊙)	L_{bol} (SED fitter)	T_{bol} (K)	α	Class	β	t (SED fitter)
0.45	6.1	3.7±0.5	2.2	51.1±1.9	0.18	flat-spectrum	0.79	148,500

3. RESULT and DISCUSSION : Dust emissivity spectral index β - 6 cores in the λ Orionis cloud

$$\frac{S_{\nu_1}}{S_{\nu_2}} = \left(\frac{\nu_1}{\nu_2}\right)^{3+\beta}\left[\frac{exp(h\nu_2/kT_d)-1}{exp(h\nu_1/kT_d)-1}\right]$$

$$\beta = \log\left[\frac{S_{\nu_1}}{S_{\nu_2}}\frac{exp(h\nu_1/kT_d)-1}{exp(h\nu_2/kT_d)-1}\right]/\log\left(\frac{\nu_1}{\nu_2}\right) - 3$$

Td: dust temperture [K]
ν1: 267.557 GHz (1.1 mm)
ν2: 230.538 GHz (1.3 mm)
$S_{\nu 1}$: peak flux density at 1.1 mm
$S_{\nu 2}$: peak flux density at 1.3 mm

	β (mean)	β (median)
SMA data	1.45	1.51
PGCC catalog for 5 PGCCS	1.83	1.81
PGCC catalog for the λ Orionis cloud	1.65	1.71

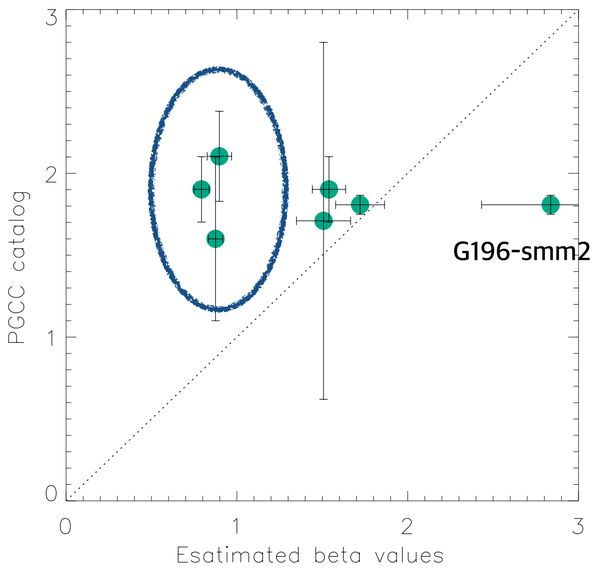

The β from PGCC catalog is plotted against the estimated β in this study.

Forbrich et al. (2015) found that β in the inner region of a starless core FeSt 1-457 shows no significant difference from the value for the local cloud, indicating that grain growth does not occur significantly in the very early stage of star formation.

I-Hsiu Li et al. (2017) , however, reported that **grain growth may reduce β in circumstellar disks or envelopes only from the late Class 0 stage to the end of the Class I stage of YSOs.**

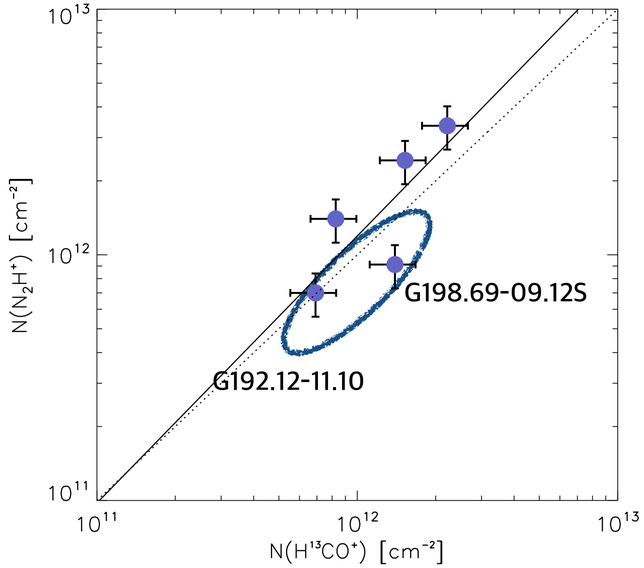

The column density of N_2H^+ is plotted against the column density of $H^{13}CO^+$.

The high density ($n \simeq 10^6$ cm^{-3}) and temperature ($T \simeq 30$ K) reached in the central core allow molecules such as CO to evaporate from grain mantles. The CO desorption causes a significant destruction of N_2H^+, which favors the formation of HCO^+.

$$N_2H^+ + CO \longrightarrow HCO^+ + N_2$$

Lee et al. 2004

4. RESULT and DISCUSSION : [HDCO]/[H_2CO] ratios with physical parameters

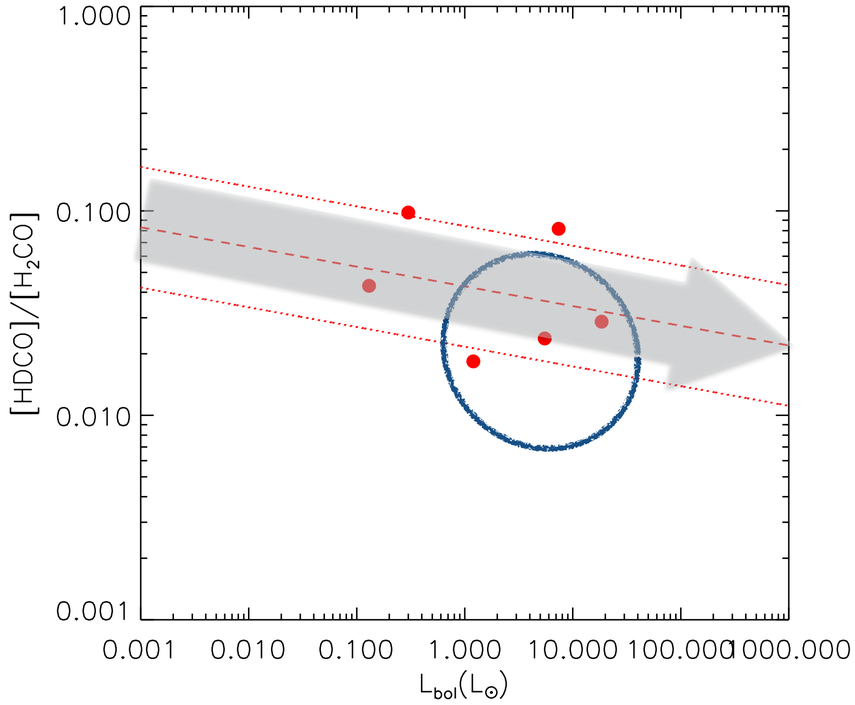

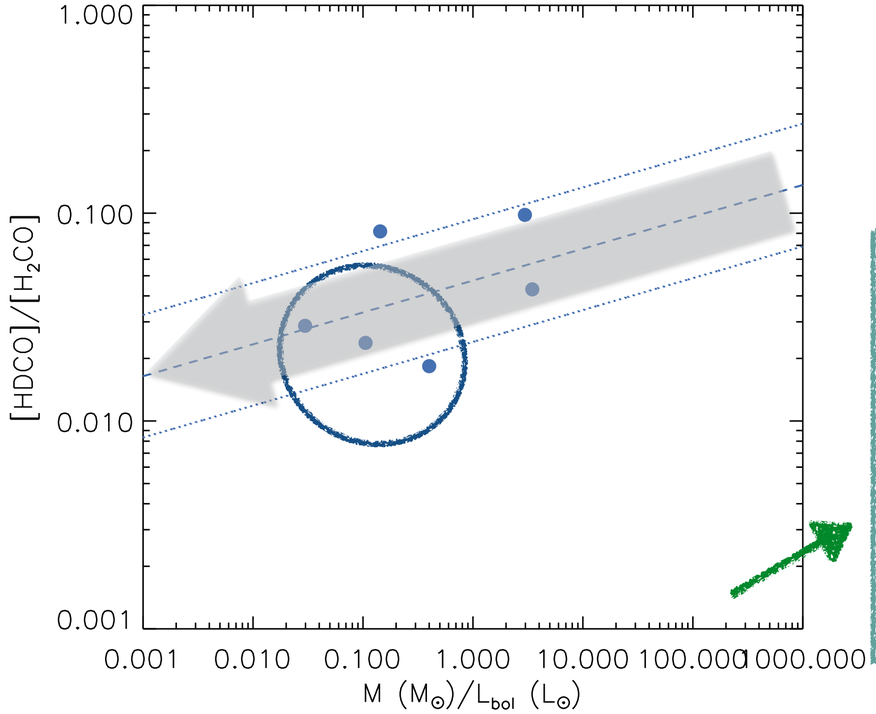

The protostellar cores with high [HDCO]/[H_2CO] ratios have relatively large mass-to-luminosity ratios, indicating that they are likely in the earliest stage of star formation.

[HDCO]/[H_2CO] ratios of 6 cores are plotted against the bolometric luminosity (L⊙) and the mass-to-bolometric luminosity ratios (M⊙/L⊙).

	G191.90	G192.12	G196.92	G198.69	G200.34N	G200.34S
N(HDCO) [10^{11} cm^{-2}]	31.1	16.6	33.2	18.4	6.0	7.1
N(H_2CO) [10^{11} cm^{-2}]	317.1	578.8	406.7	775.5	157.0	389.2
ratio (10^{-3})	98	28	82	23	43	18

5. SUMMARY

We observed 6 cores in the λ Orionis cloud with the SMA in compact configuration with ~3.0” resolution and ~0.3 mJy rms sensitivity.

For 4 objects, one component was found in each object at 1.1-mm and 1.3-mm continuum. For G196.92-10.37, dust continuum emissions show two components but for G200.34-10.97S, only 1.3-mm dust continuum show two components.

The dust spectral index, β was investigated with 1.1-mm and 1.3 mm-continuum emission. **We determine β in the range 0.79 to 2.84 for all 6 cores and find the mean value of β is 1.45 which suggest that the λ Orionis cloud was initially very dense, resulting in vigorous grain growth.**

In our previous study, **a mean value of β in the Orion A and B clouds are close to 2, while β in the λ Orionis cloud is much smaller, at 1.65. In this study for 6 cores, the mean value of β is 1.45**, which is consistent with the SCUBA-2 result.

KVN observation results are consistent with our study and well describe the stage of protostellar evolution.